Supplementary Material

Revealing the promotion of multiple Mn valences on the catalytic activity of CeO_2 nanorods toward soot oxidation

Mingyun Zhu[a], Yifeng Wen[a], Lei Shi[b], Zhiyuan Tan[a], Yuting Shen[c], Kuibo Yin[a,]*, Litao Sun[a]

[a]SEU-FEI Nano-Pico Center, Key Laboratory of MEMS of Ministry of Education, Southeast University, Nanjing, 210096, China

[b]Key Laboratory of Energy Thermal Conversion and Control of Ministry of Education, School of Energy and Environment, Southeast University, Nanjing 210096, China

[c]School of Electronic and Information Engineering, Changshu Institute of Technology, Changshu, 215500, China

*Address corresponding to: yinkuibo@seu.edu.cn

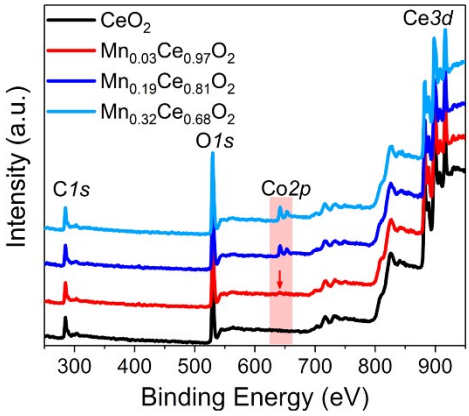

Fig. S1 Full XPS spectra of catalysts.

Table S1 Surface composition at the atomic level of the as-prepared catalysts. Data were obtained from full XPS spectra (Fig. S1).

Catalyst	O [%	Mn [%]	Ce [%]
CeO_2	76.4		23.6
$Mn_{0.03}Ce_{0.97}O_2$	76.7	0.6	22.6
$Mn_{0.19}Ce_{0.81}O_2$	76.8	4.5	18.7
$Mn_{0.32}Ce_{0.68}O_2$	83.3	5.4	11.3

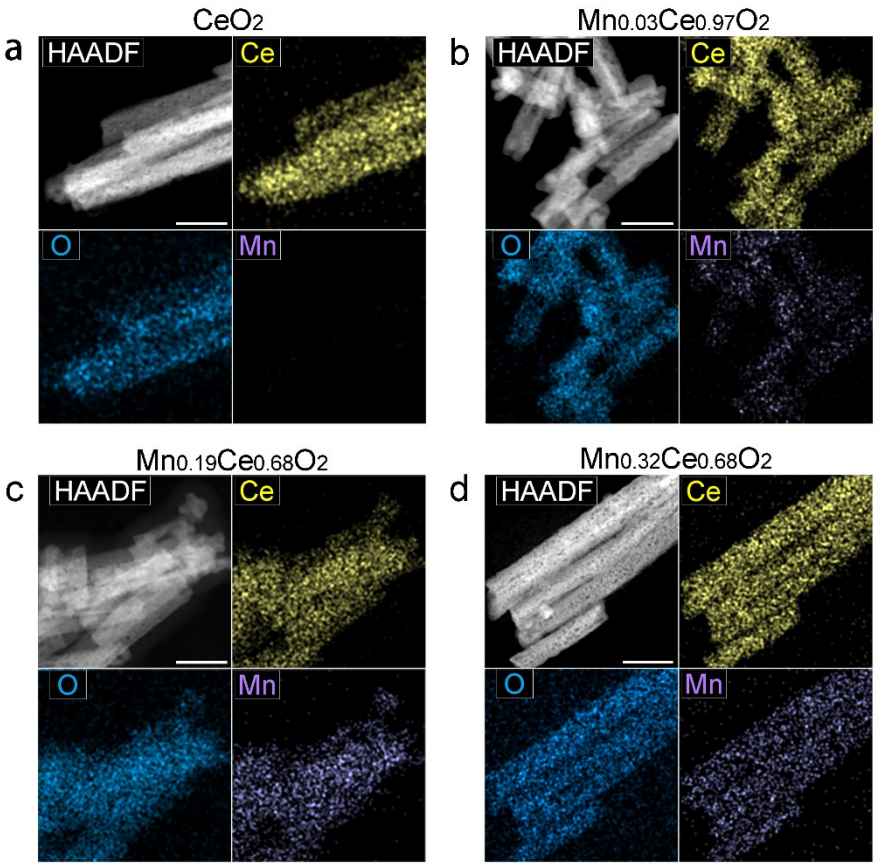

Fig. S2 STEM images of different nanorods: (a) CeO_2, (b) $Mn_{0.03}Ce_{0.97}O_2$, (c) $Mn_{0.19}Ce_{0.81}O_2$, and (f) $Mn_{0.32}Ce_{0.68}O_2$ nanorods.

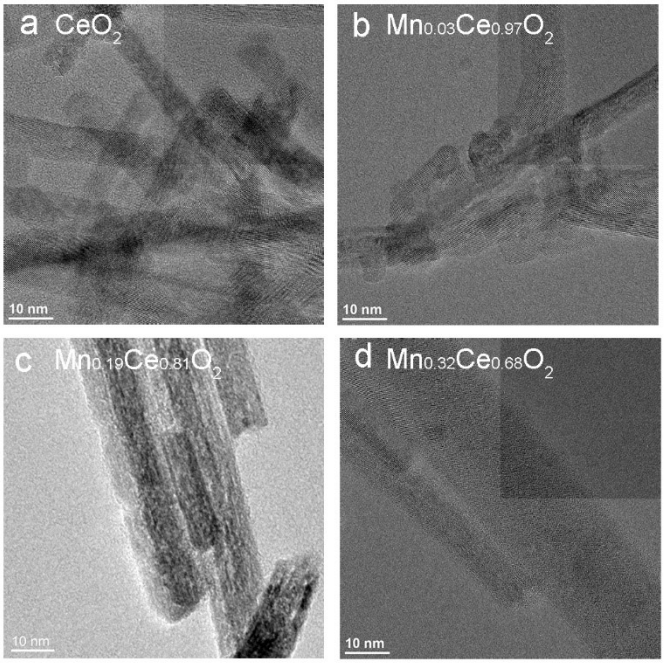

Fig. S3 TEM images of (a) CeO_2, (b) $Mn_{0.03}Ce_{0.97}O_2$, (c) $Mn_{0.19}Ce_{0.81}O_2$, (d) $Mn_{0.32}Ce_{0.68}O_2$ nanorods.

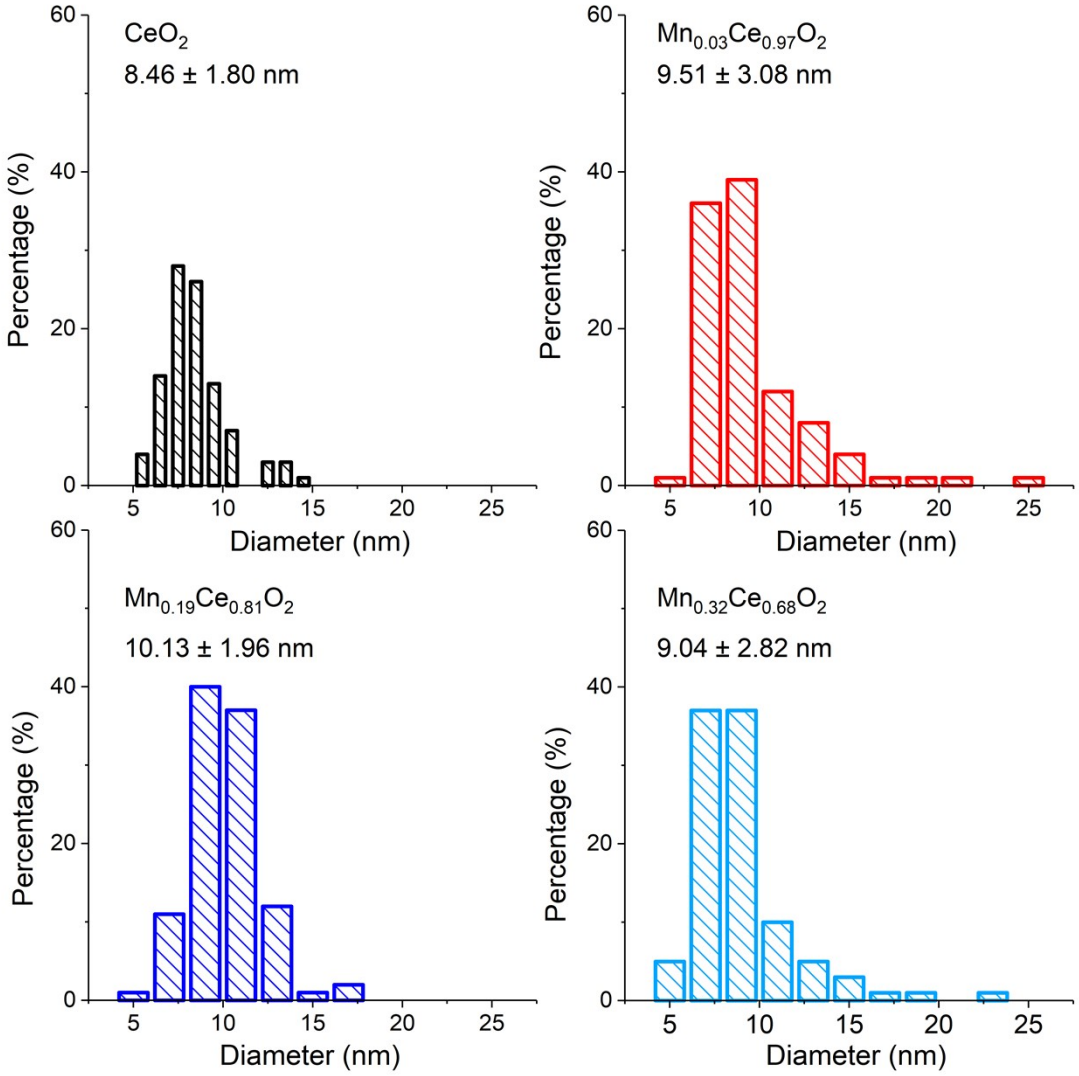

Fig. S4 Diameter distribution diagrams of different nanorods.

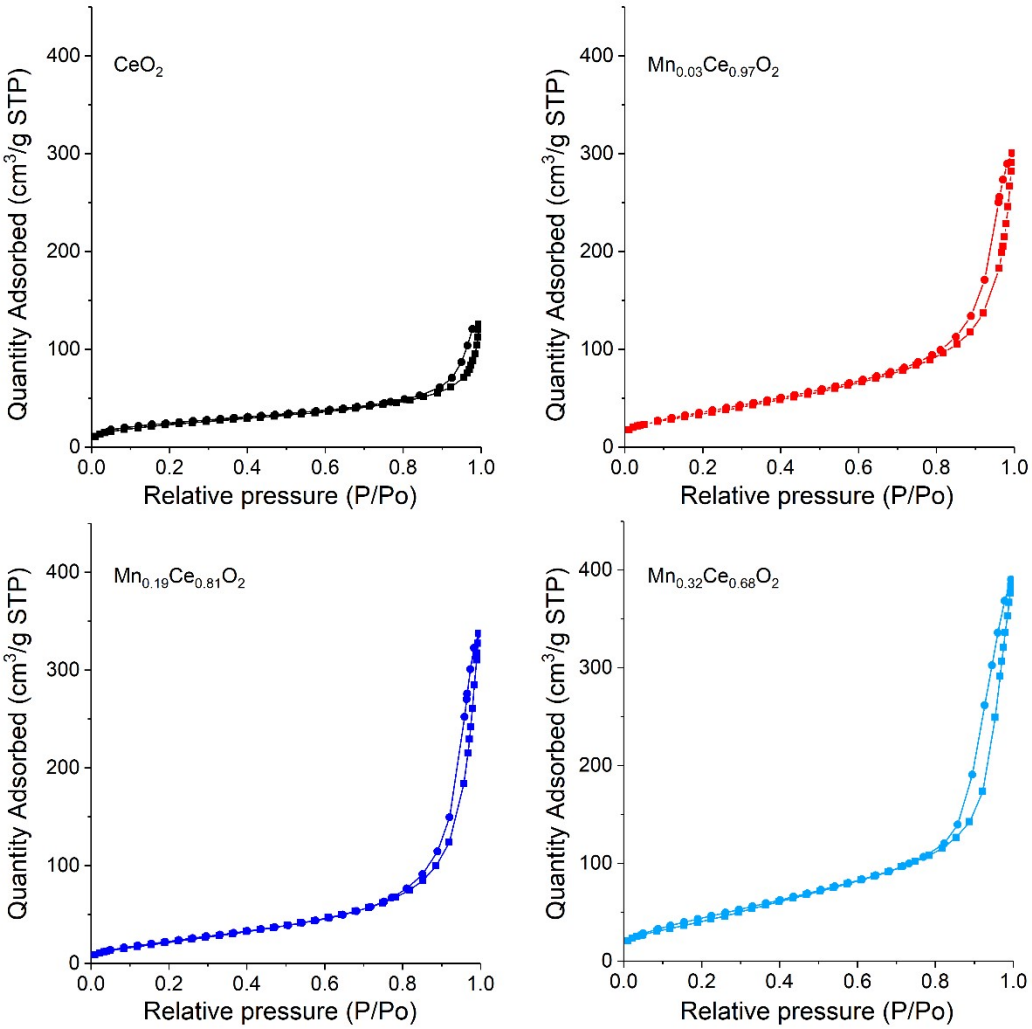

Fig. S5 Nitrogen adsorption-desorption isotherms of the as-prepared nanorods.

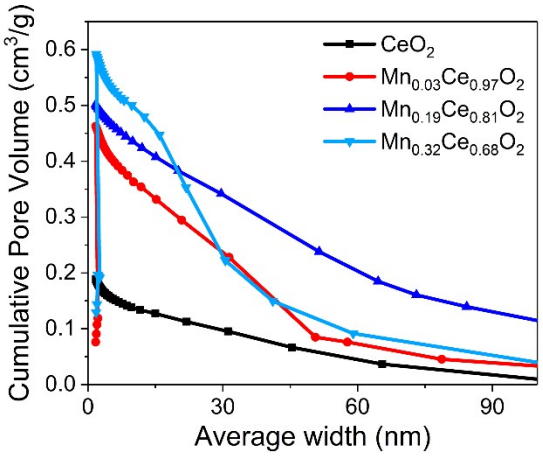

Fig. S6 Pore size distribution curves of the samples.

Table S2 Textural properties of the four catalysts.

Catalyst	S [$m^2 \cdot g^{-1}$]	V_p [$cm^3 \cdot g^{-1}$]	S_p [nm]	D_{sp} [nm]	D_n [nm]
CeO_2	82.52	0.19	9.38	1.74	8.46 ± 1.80
$Mn_{0.03}Ce_{0.97}O_2$	126.11	0.46	11.35	1.74	9.51 ± 3.08
$Mn_{0.19}Ce_{0.81}O_2$	83.99	0.52	17.06	1.74	10.13 ± 1.96
$Mn_{0.32}Ce_{0.68}O_2$	154.62	0.59	12.34	1.88	9.04 ± 2.82

S: specific surface area which is calculated by BET method.

V_p: pore volume which is calculated by BJH desorption cumulative volume of pores between 1.7 nm and 300 nm diameter.

D_{sp}: stacking pore diameter which is determined by BJH desorption average pore diameter.

S_p: pore size within nanorods which is obtained from pore size distribution curves in Fig. S6.

D_n: the average diameter of nanorods which is collected by STEM images in Fig. S2.

Table S3 Catalytic performances of the as-prepared catalysts toward soot combustion in 5%H_2O/10%O_2/N_2 and the comparation with other catalysts.

Catalyst	Gas environment	Heating rate [°C/min]	T_{50} [°C]	CO_2 selectivity [%]	Ref.
CeO_2	5%H_2O/O_2/N_2	5	513	96%	This work
$Mn_{0.03}Ce_{0.97}O_2$	5%H_2O/O_2/N_2	5	499	100%	
$Mn_{0.19}Ce_{0.81}O_2$	5%H_2O/O_2/N_2	5	464	100%	
$Mn_{0.32}Ce_{0.68}O_2$	5%H_2O/O_2/N_2	5	490	99%	
$Fe/Ce_{0.9-x}Zr_{0.1}O_x$	5%H_2O/NH_3/NO/O_2/N_2	3	421		[1]
K-OMS-2/TSO	10%H_2O/NO/O_2/Ar	2	~335	~98%	[2]
$K_xMn_8O_{16}/Mg_2Al_4Si_5O_{18}$	10%H_2O/NO/O_2/N_2		405	100%	[3]
$Ag/SmMn_2O_5$	5%H_2O/NO/O_2/N_2		470	100%	[4]

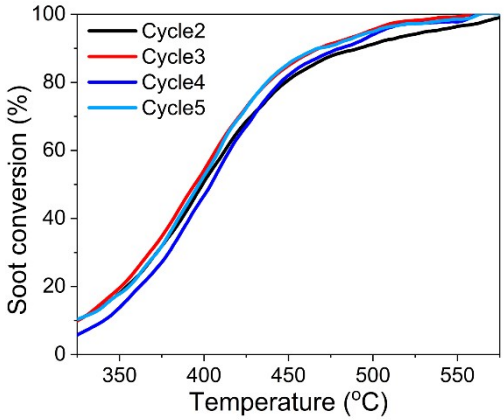

Fig. S7 Consecutive soot conversation curves over $Mn_{0.19}Ce_{0.81}O_2$ catalyst under a loose contact condition in air.

Table S4 Catalytic stability of $Mn_{0.19}Ce_{0.81}O_2$ nanorods.

Reaction cycle	1st	2nd	3rd	4th	5th
T_{50} [°C]	356	399	394	403	396

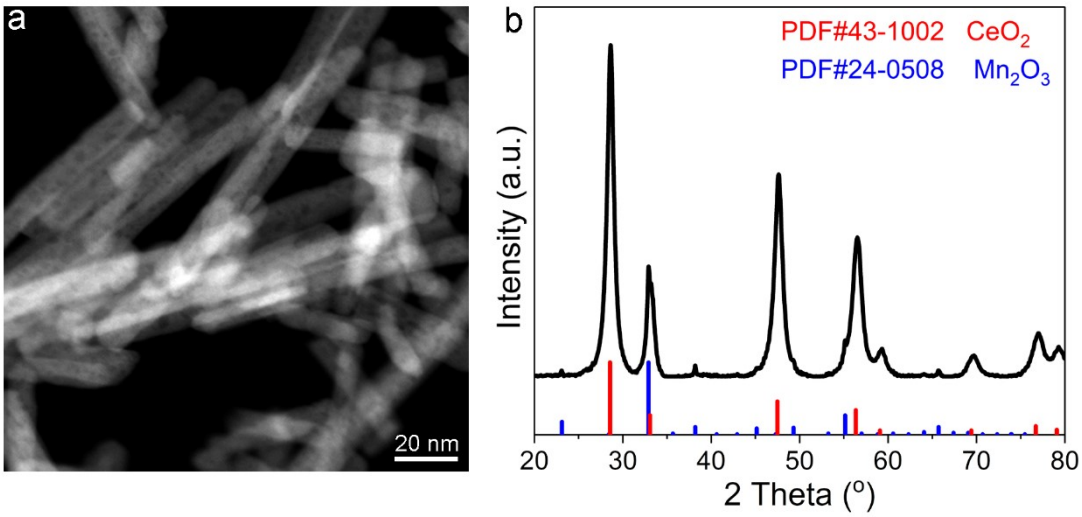

Fig. S8 (a) STEM image and (b) XRD pattern of the aged $Mn_{0.19}Ce_{0.81}O_2$ catalyst.

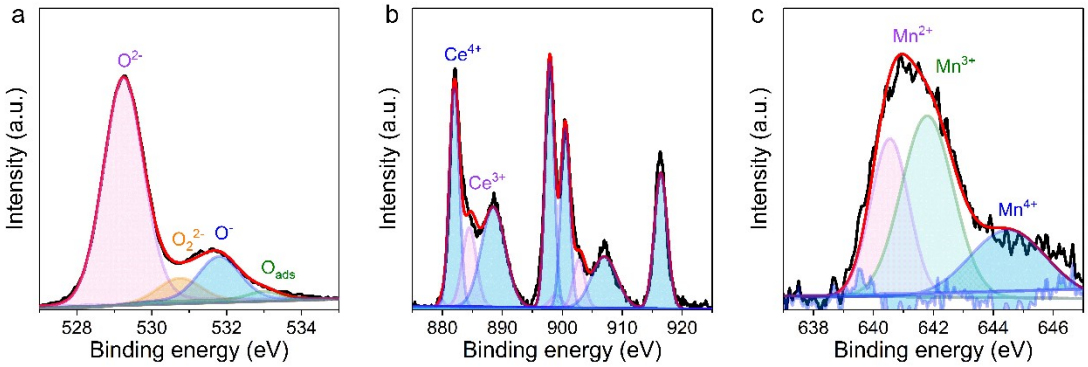

Fig. S9 (a) O*1s*, (b) Ce*3d* and (c) Mn*2p* XPS spectra of $Mn_{0.19}Ce_{0.81}O_2$ catalyst after reaction 5 cycles.

Table S5 Surface composition and chemical states of O*1s*, Ce*3d*, and Mn*2p* species within the aged $Mn_{0.19}Ce_{0.81}O_2$.

Catalyst	O species [%]		Ce species [%]		Mn species [%]		
	O^{2-}	P_o	Ce^{3+}	Ce^{4+}	Mn^{2+}	Mn^{3+}	Mn^{4+}
$Mn_{0.19}Ce_{0.81}O_2$	75.6	24.4	23.0	77.0	29.2	45.6	25.2

P_o: chemically and physically adsorbed oxygen species.

Results are derived from XPS analyses (Fig. S9).

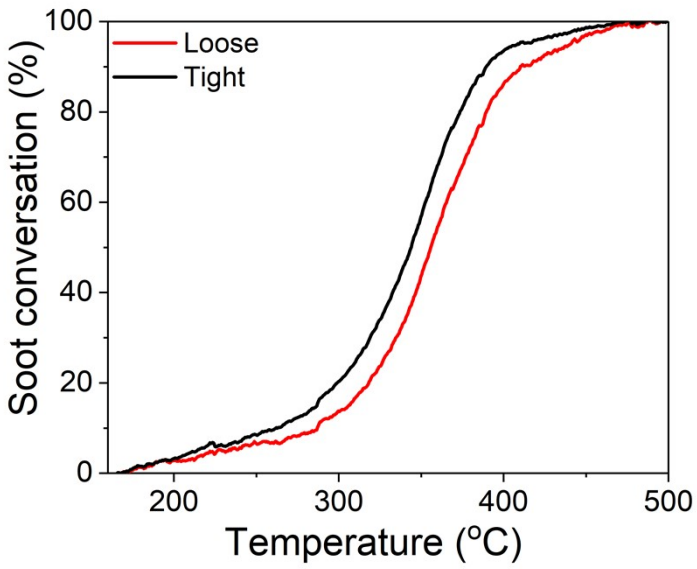

Fig. S10 Soot conversation curves over the $Mn_{0.19}Ce_{0.81}O_2$ under different contact conditions in air. In tight condition, 10.0 mg catalysts and 1.0 mg soot nanoparticles were ground for 2 min.

Table S6 Catalytic performances of the $Mn_{0.19}Ce_{0.81}O_2$ catalyst under different contact conditions.

Contact condition	T_{10} [°C]	T_{50} [°C]	T_{90} [°C]
Loose	287	356	410
Tight	262	343	388

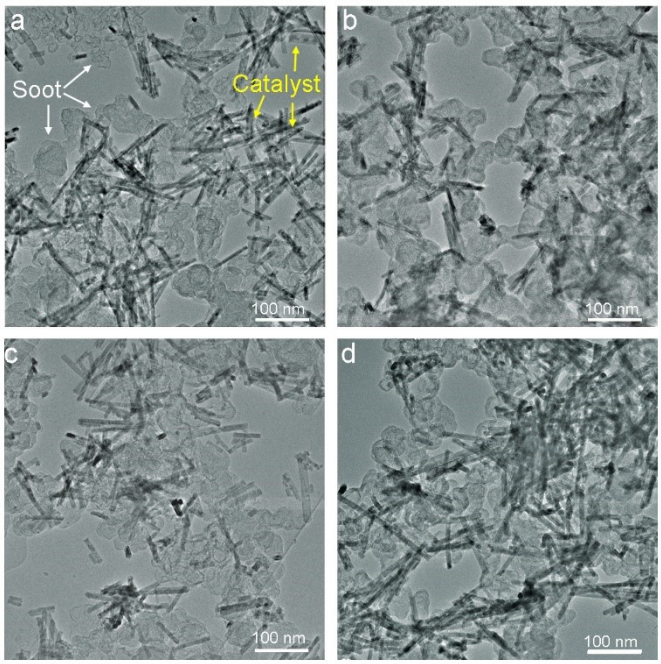

Fig. S11 TEM images of the soot particles contacting with (a) CeO_2, (b) $Mn_{0.03}Ce_{0.97}O_2$, (c) $Mn_{0.19}Ce_{0.81}O_2$, (d) $Mn_{0.32}Ce_{0.68}O_2$ nanorods.

Theoretical calculation

Interaction energies (E_{int}) between C and catalysts as well as between O_2 and catalysts were calculated using the Forcite Plus package in BIOVIA® Materials Studio at the level of the molecular mechanics.[5, 6] The employed CeO_2{111}, {220}, and {200} surfaces with (3×3) supercells contain 90, 135, and 90 atoms, respectively. The Mn-modified structural models were realized by replacing the lattice Ce with Mn or adding the Mn over the lattice surface. The energetic simulation was carried out under the condition of constant 298 K using the Universal forcefield with the Ewald electrostatic interaction. The accessible accuracy was maintained at 10^{-5} kcal·mol^{-1}. The E_{int} was derived by:

$$E_{int} = E_{total} - E_{sub} - E_{mol}$$

In the above equation, E_{int} is the resulting interaction energies of C and/or O_2, E_{total} the total energy of the entire system, E_{sub} the energy of the substrate, E_{mol} the energy of C or O_2 molecules.

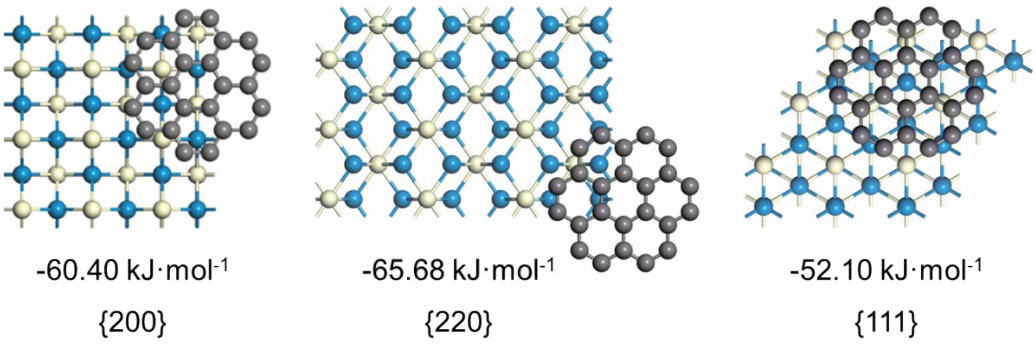

Fig. S12 Models of the final configurations used to calculate the interaction energy (E_{int}) between C and the CeO_2 {200}, {220} or {111} facets. The light yellow and blue balls are the lattice Ce and O atoms within CeO_2 and the grey ball are C atoms within soot particles. The next texts will not explain these colorful balls.

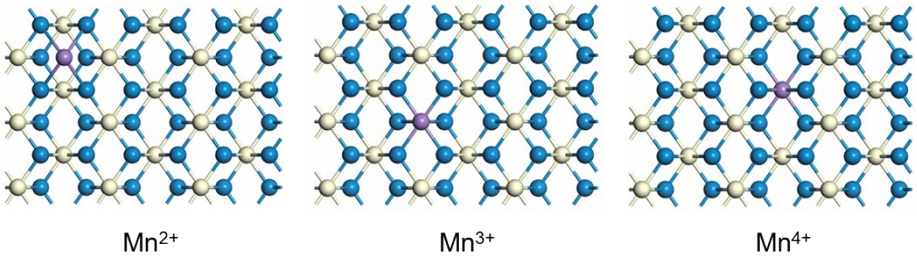

Fig. S13 The employed models of CeO_2 {220} facet with the (left) Mn^{2+}, (medium) Mn^{3+} and (right) Mn^{4+} doping. The light purple balls are the Mn heteroatoms, which will not be explained in the next text.

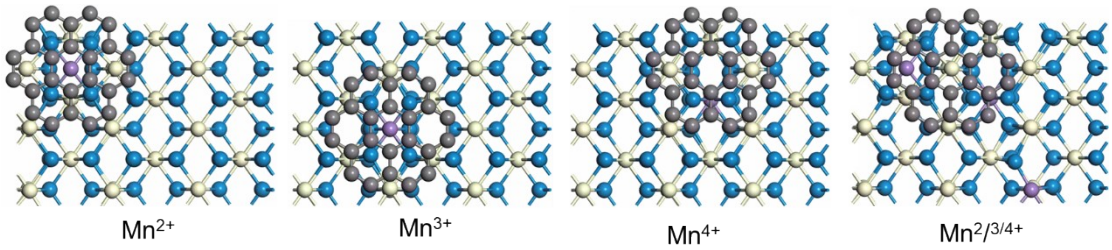

Fig. S14 The optimized structures of C on CeO_2 {220} facet with the Mn-modified.

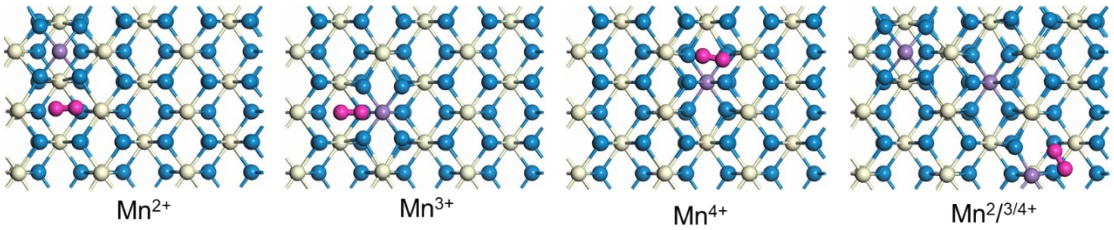

Fig. S15 The optimized structures of O_2 on CeO_2 {220} facet with the Mn-modified. Purple balls: O atoms in oxygen molecules.

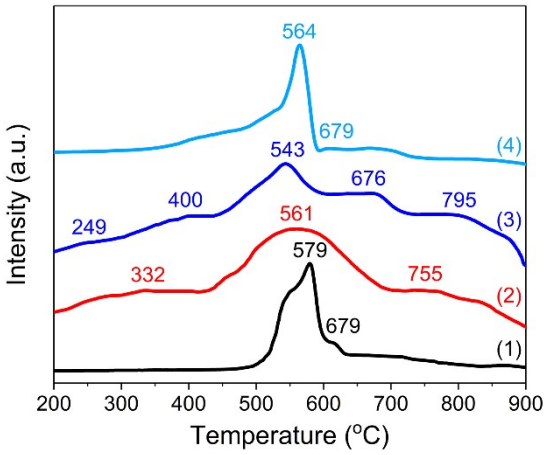

Fig. S16 O_2-TPD profiles of the samples: (1) CeO_2, (2) $Mn_{0.03}Ce_{0.97}O_2$, (3) $Mn_{0.19}Ce_{0.81}O_2$, (4) $Mn_{0.32}Ce_{0.68}O_2$.

Refences

1. Y. Cheng, W. Song, J. Liu, H. Zheng, Z. Zhao, C. Xu, Y. Wei and E. J. M. Hensen, *ACS Catal*, 2017, **7**, 3883-3892.
2. X. Yu, Y. Ren, D. Yu, M. Chen, L. Wang, R. Wang, X. Fan, Z. Zhao, K. Cheng, Y. Chen, J. Gryboś, A. Kotarba, Z. Sojka, Y. Wei and J. Liu, *ACS Catalysis*, 2021, **11**, 5554-5571.
3. Y. Yang, D. Zhao, Z. Gao, Y. Tian, T. Ding, J. Zhang, Z. Jiang and X. Li, *Applied Catalysis B: Environmental*, 2021, **286**, 119932-119942.
4. B. Jin, B. Zhao, S. Liu, Z. Li, K. Li, R. Ran, Z. Si, D. Weng and W. Xiaodong, *Applied Catalysis B: Environmental*, 2020, **273**, 119058-119067.
5. M. Zhu, Y. Wen, S. Song, A. Zheng, J. Li, W. Sun, Y. Dai, K. Yin and L. Sun, *Nanoscale*, 2020, **12**, 19104-19111.
6. M. Zhu, K. Yin, Y. Wen, S. Song, Y. Xiong, Y. Dai and L. Sun, *Nano Research*, 2021, DOI: 10.1007/s12274-021-3659-6.